Solution-processed cavity and slow-light quantum electrodynamics in near-infrared silicon photonic crystals

R. Bose, J. F. McMillan, J. Gao, and C. W. Wong

Related Articles

Generalized channels: Channels for convex subsets of the state space
J. Math. Phys. 53, 012201 (2012)

Invited Review Article: Single-photon sources and detectors
Rev. Sci. Instrum. 82, 071101 (2011)

Cascading dynamics in complex quantum networks
Chaos 21, 025107 (2011)

Electron spin ensemble strongly coupled to a three-dimensional microwave cavity
Appl. Phys. Lett. 98, 251108 (2011)

Capacities of Grassmann channels
J. Math. Phys. 52, 062202 (2011)

Additional information on Appl. Phys. Lett.

Journal Homepage: http://apl.aip.org/

Journal Information: http://apl.aip.org/about/about_the_journal

Top downloads: http://apl.aip.org/features/most_downloaded

Information for Authors: http://apl.aip.org/authors

Solution-processed cavity and slow-light quantum electrodynamics in near-infrared silicon photonic crystals

R. Bose,[a)] J. F. McMillan,[b)] J. Gao,[c)] and C. W. Wong[a)]

Optical Nanostructures Laboratory, Center for Integrated Science and Engineering, Solid-State Science and Engineering and Mechanical Engineering, Columbia University, New York, New York 10027, USA

We demonstrate enhanced emission of solution-processed sparse lead sulfide quantum dots (QDs) coupled to confined as well as propagating modes in silicon photonic crystals at near-infrared communications wavelengths. In the cavity case, by using cold-cavity characterization using on-board waveguides or cross-polarization techniques, we show that the coupled QD lineshape is identical to the cold-cavity spectra. For the photonic crystal waveguides (PhCWGs), we use transmission spectra for the PhCWG as well as three-dimensional finite difference time domain techniques to validate enhancements due to the propagating mode. The observation of room-temperature quantum electrodynamics using postfabrication QD integration techniques is promising for further studies. © *2009 American Institute of Physics.* [doi:10.1063/1.3238555]

Semiconductor quantum dots (QDs), made up of thousands of atoms and exhibiting highly quantized, atomlike levels have emerged as strong contenders for studying cavity quantum electrodynamics (QED)[1–3] in the solid state. Coupling QD to localized[4,5] or propagating modes[6] in photonic crystals (PhCs) overcomes problems of quantum decoherence through interactions with the PhC modes allowing remarkable experimental possibilities. Solution-processed lead-salt QDs, such as PbS and CdSe, are especially attractive because they offer possibilities of postfabrication positioning and integration. In particular, PbS QDs are promising due to their wavelength compatibility with the highly developed silicon complementary metal-oxide-semiconductor (CMOS) infrastructure that allow them to be used for studying QD interactions with cavity or waveguide modes in two-dimensional (2D) PhC utilizing postfabrication integration techniques. In this work, we present coupling of monolayer PbS QDs[7–9] in low densities to nominally perturbed silicon PhC cavities with modes supporting Q around 1000, as well as slow-light ($<c/4$) PhC waveguide (PhCWG) modes with considerable enhancement contrasts over uncoupled dots.

In order to characterize the optical properties of the silicon PhCs, we use various active and passive experimental techniques (such as cross polarization[10]) that are summarized in Fig. 1(a). PbS QDs on the device surface are used to study quantum interactions in the cavity and waveguide regions, and actively characterize the system. The QDs, synthesized using traditional methods,[11] are suspended in a chloroform solution and exhibit room-temperature photoluminescence (PL) centered at 1470 nm with a full width half maximum of ~150 nm due to size dispersity. The QDs (from Evident Technologies) are spin-coated on the devices in sparse densities (100–250 μm^{-2}) and vertically pumped using a 980 nm diode laser (up to 60 mW). The typical lifetimes for the QDs (~100 ns in film[12]) make the detection of single QDs

challenging but can be enabled by cavity QED enhancement, improved collection methods such as with tapered fiber spectroscopy[13] or cavity design,[14] higher quantum efficiencies, or improved detectors.

The devices studied here are silicon-on-insulator (SOI) PhC [Fig. 1(b)] with a linear defect ($L3$-type) cavity. The triangular lattice 2D PhC has lattice period $a=420$ nm, air hole-radius $r=0.29a$, and thickness t of 250 nm for the silicon slab. The holes adjacent to the cavity region are modified ($s=0.15a$) to improve the cavity Q factors as in Ref. 15. The cavity modes and parameters are calculated using three-dimensional (3D) finite difference time domain (FDTD) with subpixel accuracy.[16] The samples are fabricated in a CMOS foundry, with low (sub-20 Å) statistically quantified disorder.[17] Using cross-polarization measurements, Qs between 250 and 7500 are observed for the cavity modes with QDs spun on the surface. Using scanning electron microscopy (SEM), we locate the positions of single QDs [Fig. 1(b)], allowing us to estimate the number of QDs that can couple to the cavity mode. The estimated Purcell factors[18] range between 7 and 200 in the cavity-limited coupling regime for the above passive measurements of the cavity mode.

Figure 1(c) shows the coupling of PbS QDs to confined modes of a $L3$ cavity with different design radii, exhibiting Q factors of around 250. The observed resonances can be confirmed using cross-polarization characterization (gray) of the cavities as shown in the figure. Due to the low quality factors, the maximum Purcell factors are limited to around ~7. This number is further lowered due to the constraint of evanescent coupling. However, we may infer from the high enhancement intensity contrasts of 12× of the cavity-coupled dots that only a few QDs are selectively coupled to the cavity mode. It should be emphasized that the current $L3$ cavity mode exhibits low outcoupling efficiencies (objective lens NA=0.7; estimated around ~5%). In Fig. 1(c), we note also the emergence of a second mode that is blueshifted by 10 nm from the fundamental cavity mode. Using cross-polarization measurements on devices without QD [inset of Fig. 1(c)], we confirm that a second closely spaced mode exists close to the fundamental resonance of the cavity, veri-

---
a)Authors to whom correspondence should be addressed. Electronic addresses: rb2261@columbia.edu. Tel.: 212-854-7253 and cww2104@columbia.edu. Tel.: 212-854-4275.
b)Electronic mail: jfm2113@columbia.ed. Tel.: 212-854-7253.
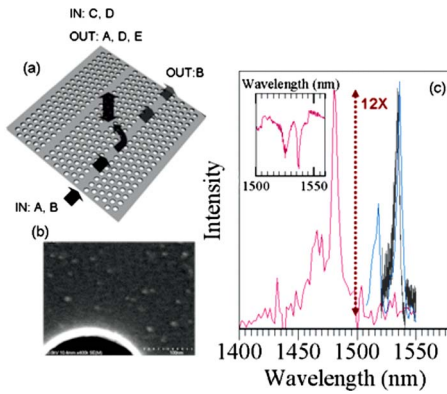c)Electronic mail: jg2499@columbia.edu. Tel.: 212-854-7253.

FIG. 1. (Color online) (a) Schematic of measurement schemes used in this work. (i) Cavity radiation, where a tunable laser source (a) is coupled through the waveguide and the cavity radiation collected from the top of the device. (ii) Waveguide transmission where a supercontinuum laser source (b) is used. (iii) Cross polarization, where the tunable laser source (d) is coupled to the cavity mode vertically, and the radiation are also collected in the same direction (reflection). (iv) QD PL either at the cavity or waveguide regions, where a 980 nm diode laser (c) is used to excite the QD vertically and the QD radiation is collected from the top (e). (b) SEM image of a typical $L3$ PhC shown with single QDs (6 nm diameter) on the surface. Scale bar: 100 nm. (c) QD characterization of cavity modes for different filling factors ($r_1 = 0.29a$, $r_2 = 0.3523a$), along with a cross-polarization measurement (gray, high resolution). Device Qs are around 250. (Inset) Cross-polarization spectroscopy of device without dots shows two closely spaced modes ($\Delta\lambda = 10$ nm).

fying the additional features in the PL spectra.

Devices with on-board PhCWGs enable advanced single cavity as well as multicavity interactions with QDs, as well as slow-light propagating modes that support high Purcell factors.[19] The coupling of QD to propagating modes in the PhCWG is especially interesting in the case where quantum interactions between the QD exciton and photons need not be confined in the limited spatial extent of the cavity, thereby relaxing requirements for spatial matching of QD to the cavity field maxima, and circumvents additional out-coupling losses due to the cavity for single-photon source applications.[19]

Even at the sparse QD levels, we clearly observe the signatures of the PhCWG cavity mode (~1548 nm, Fig. 2),
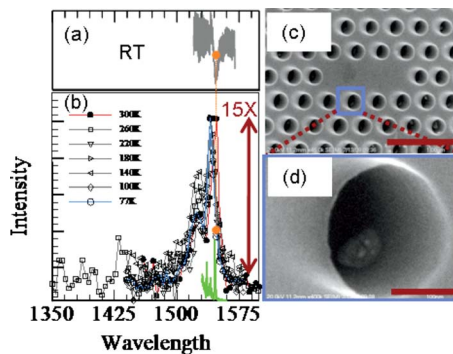

FIG. 2. (Color online) Coupled QD-cavity measurements for a PhC cavity mode in a PhCWG device. (a) Cross-polarization spectroscopy (blue) showing a non-Lorentzian lineshape at the cavity resonance. (b) Waveguide characterization (green, lower-most spectrum, at room temperature) and QD PL showing signatures of the cavity mode at room and cryogenic temperatures. (c) SEM of dots at the cavity showing very few dots on the device surface and few QDs along the hole sidewalls and at the bottom interface. (d) One of the PhC holes is shown in detail where three single QD can be clearly seen from the SEM. Scale bars: 1 μm in (c) and 100 nm in (d).
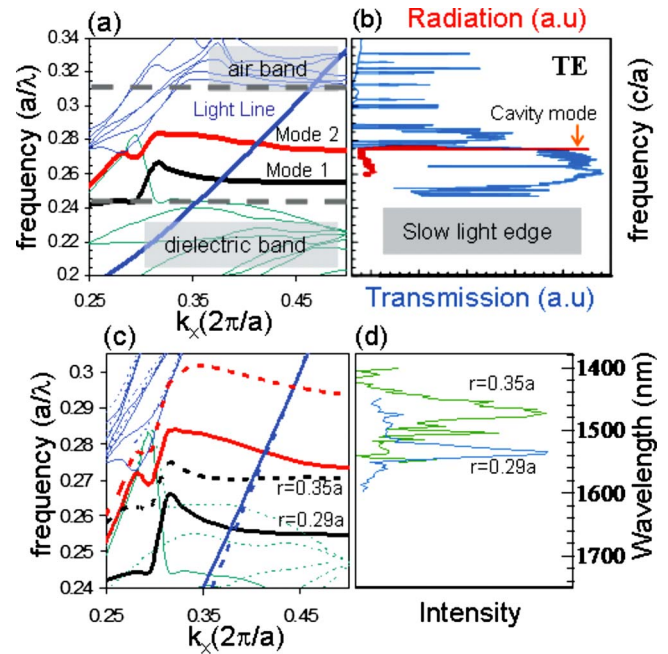

FIG. 3. (Color online) (a) Projected band structure for a SOI PhCWG with hole radius of $0.29a$, with the dielectric (green) and air (blue) bands shown. The blue thick slanted line represents the light line. The fundamental and second order TE propagating modes are shown in black and red, respectively, and both modes exhibit near-flat dispersion at the mode onsets, allowing for enhanced light-matter interactions. (b) TE transmission for a device with the parameters used in (a) and containing QDs on the surface showing good agreement with the projected band structure. The cavity mode is shown in red. (c) Projected band structures for design radii of $0.29a$ (solid) and $0.3523a$ (dashed) showing the shifts in the band structure features. (d) Waveguide enhancements for QD emission coupled to the second-order (odd) PhCWG modes for both design radii, showing a shift of 60 nm between the two cases.

as well as the blueshifted second mode, that are confirmed in both waveguide and cross-polarization measurements (the cross-polarization measurement in this case exhibits a non-Lorentzian lineshape but confirms the cavity resonance wavelength). The cavity quality factor measured from the passive waveguide spectrum is ~1000, allowing Purcell factors of ~30 at the cavity field maximum. The number of dots that can couple into the cavity mode depends largely on the single dot linewidths. At room temperature, where dephasing effects broaden the QD linewidths, QDs that are away from the cavity resonance can still couple with the cavity mode through phonon mediated coupling, leading to an effective photon-transfer process in the context of PhC-based single-photon sources.[3] SEM of the devices [Fig. 2(c)] shows low density of dots at the device surface (<200 μm^2), although dots can be observed along the sidewalls and at the SiO$_2$/Si interface [Fig. 2(d)] (this density is also very low). We further tune the temperature of our sample from room temperature to 77 K using a liquid nitrogen cryostat chamber, but do not observe any remarkable effects of temperature tuning, other than a blueshift in the cavity resonance with decreasing temperature of about 8 nm. Conversely, the QD ensemble-resonance shifts by +80 nm and narrows to a linewidth of ~100 nm, offering different QDs for coupling to the same cavity mode. This universal performance of the lead-salt QDs is distinctly different from III-V semiconductor QDs.

Figure 3(a) shows the projected band structure for the PhCWG using 3D FDTD.[20] The transverse-electric polariza-

tion (TE) bandgap occurs between normalized frequencies of 0.24 and 0.315 $[a/\lambda]$ (corresponding to between 1330 and 1750 nm) with two TE line-defect propagating modes with slow-light mode onsets at 0.255 and 0.273 $[a/\lambda]$, respectively (corresponding to 1647 and 1539 nm). In our experiments, as we move the micro-PL collection region from the PhC cavity to different regions on the PhCWG, we observe high enhancements in a spectral region that is 10 nm blueshifted from the cavity resonance, with a ~16 nm bandwidth. This identical resonance (TE-polarized) is observed in all regions along the PhCWG confirming that the enhancement is due to QD coupling to a propagating PhCWG mode, with an estimated group velocity of $c/4$. Correspondingly, there is no observation of QD enhanced emissions anywhere in the PhC region, confirming that the effect is limited to the waveguide region. The position of this enhancement region with respect to the cavity mode suggests that the PbS QD coupling is indeed with the higher-order TE band (shown in red). In order to further confirm these observations, we characterize TE propagating modes in waveguide transmission measurements, as shown in the experimental results of Fig. 3(b), for a device with sparse QDs, and supporting a measured mode with Q of 7500 (shown in red) and representative of devices with $r=0.29a$. Indeed we find that the slow-light region of the first order PhCWG mode occurs at over 100 nm longer wavelength than the cavity mode, whereas the PhCWG second order mode onset lies very close to the cavity mode from our projected band structure calculations. As a further confirmation, we study slow-light enhancements in a PhCWG device with a radius that is 18% larger [Figs. 3(c) and 3(d)] than the previous example, and observe an enhancement region [Fig. 3(d)] that is 60 nm blueshifted compared to the case where $r=0.29a$. Simulations of the projected band structure show a very similar shift for the second order mode onset, and any discrepancies are within the computational errors. Coupling of QDs to this fundamental mode is not generally observed due to this region being outside our experimental range.

The Purcell factors in the PhCWG region may be calculated using Green's function tensor formalism[19] for QDs placed on the slab surface, and a maximum Purcell factor value of ~9 is derived at the optimal emitter position on the device surface for the parameters shown in the experiments. The computed resonance linewidths are in agreement with our observations and are determined by the slow-light edges and the light line.

In conclusion, we present observations of QD coupling using sparse PbS QDs on silicon PhCs. By employing passive techniques to characterize the devices without the need for a waveguide, we show that the QD-coupled spectrum decorates the cavity spectrum at room and cryogenic temperatures. We further demonstrate efficient QD coupling to the higher order propagating TE waveguide mode in a PhCWG at the slow-light edge.

[1]H. Mabuchi and A. C. Doherty, Science **298**, 1372 (2002).
[2]D. Bouwmeester and A. Zeilinger, *The Physics of Quantum Information* (Springer, Berlin, 2000).
[3]A. Auffèves, J.-M. Gérard, and J.-P. Poizat, Phys. Rev. A **79**, 053838 (2009).
[4]A. Faraon, I. Fushman, D. Englund, N. Stoltz, P. Petroff, and J. Vučković, Nat. Phys. **4**, 859 (2008).
[5]G. Khitrova, H. M. Gibbs, M. Kira, S. W. Koch, and A. Scherer, Nat. Phys. **2**, 81 (2006).
[6]T. Lund Hansen, S. Stobbe, B. Julsgaard, H. Thyrrestrup, T. Sünner, M. Kamp, A. Forchel, and P. Lodahl, Phys. Rev. Lett. **101**, 113903 (2008).
[7]I. Fushman, D. Englund, and J. Vučković, Appl. Phys. Lett. **87**, 241102 (2005).
[8]R. Bose, X. Yang, R. Chatterjee, J. Gao, and C. W. Wong, Appl. Phys. Lett. **90**, 111117 (2007).
[9]Z. Wu, Z. Mi, P. Bhattacharya, T. Zhu, and J. Xu, Appl. Phys. Lett. **90**, 171105 (2007).
[10]P. B. Deotare, M. W. McCutcheon, I. W. Frank, M. Khan, and M. Loncar, Appl. Phys. Lett. **94**, 121106 (2009).
[11]M. A. Hines and G. D. Scholes, Adv. Mater. (Weinheim, Ger.) **15**, 1844 (2003).
[12]R. Bose, J. F. McMillan, J. Gao, C. J. Chen, D. V. Talapin, C. B. Murray, K. M. Rickey, and C. W. Wong, Nano Lett. **8**, 2006 (2008).
[13]K. Srinivasan and O. Painter, Nature (London) **450**, 862 (2007).
[14]N.-V.-Q. Tran, S. Combrié, and A. De Rossi, Phys. Rev. B **79**, 041101(R) (2009).
[15]Y. Akahane, T. Asano, B.-S. Song, and S. Noda, Nature (London) **425**, 944 (2003).
[16]A. Farjadpour, D. Roundy, A. Rodriguez, M. Ibanescu, P. Bermel, J. D. Joannopoulos, S. G. Johnson, and G. Burr, Opt. Lett. **31**, 2972 (2006).
[17]R. Chatterjee, N. C. Panoiu, K. Liu, Z. Dios, M. Yu, M. T. Doan, L. J. Kaufman, R. M. Osgood, and C. W. Wong, Phys. Rev. Lett. **100**, 187401 (2008).
[18]E. M. Purcell, Phys. Rev. **69**, 37 (1946).
[19]V. S. C. Manga Rao and S. Hughes, Phys. Rev. B **75**, 205437 (2007).
[20]S. G. Johnson and J. D. Joannopoulos, Opt. Express **8**, 173 (2001).